Acknowledgment

We thank Professor Roger G. Bates for helpful comments.

Literature Cited

(1) Covington, A. K.; Bates, R. G.; Durst, R. A. *Pure Appl. Chem.* **1983**, *55*, 1467.
(2) Mussini, T.; Covington, A. K.; Longhi, P.; Rondinini, S. *Pure Appl. Chem.* **1985**, *57*, 865.
(3) White, D. R.; Warner, P. *J. Chem. Eng. Data* **1988**, *33*, 174.
(4) Bates, R. G. *Determination of pH*, 2nd ed.; Wiley: New York, 1973; Chapter 10.
(5) Bates, R. G.; Guggenheim, E. A. *Pure Appl. Chem.* **1960**, *1*, 163.
(6) Mussini, T.; Cicognini, M.; Longhi, P.; Rondinini, S. *Anal. Chim. Acta* **1984**, *162*, 103.
(7) Mussini, T.; Longhi, P.; Rondinini, S.; Tettananti, M.; Covington, A. K. *Anal. Chem. Acta* **1985**, *174*, 331.
(8) Bates, R. G.; Bennetto, H. P.; Sankar, M. *Anal. Chem.* **1980**, *52*, 1598.
(9) Bates, R. G. *J. Am. Chem. Soc.* **1948**, *70*, 1579.

Received for review September 19, 1988. Accepted April 11, 1989.

Surface Tension and Electrical Conductivity of Molten Thiocyanates MSCN (M = Na, K, Rb, and Cs)

Kazuo Igarashi* and Junichi Mochinaga

Department of Synthetic Chemistry, Faculty of Engineering, Chiba University, Chiba-shi, Chiba 260, Japan

Surface tensions and electrical conductivities of molten thiocyanates MSCN (M = Na, K, Rb, and Cs) have been measured by the maximum bubble pressure method and the ac bridge method, respectively, and their values were expressed as functions of temperature. Both results for MSCN melts were found to be close to those of typical ionic melts such as nitrates and halides.

Introduction

A linear SCN^- ion is present in alkali-metal thiocyanate melts near their melting points (*1–3*) as well as in the solid state (*4–8*). Physicochemical properties of the melts with such an ion are of interest in the comparison with those of alkali-metal halide and nitrate melts. Some properties for molten potassium and sodium thiocyanates have been reported by Ubbelohde et al. (*9*, *10*), Jindal and Harrington (*11*), and Cingolani et al. (*12*). However, there are little data reported on the other alkali-metal thiocyanate melts. In order to systematically study properties of the melts, we measured the densities and refractive indexes of a series of alkali-metal thiocyanate melts (*13*) and evaluated an electronic polarizability of SCN^- ion in the molten state using their results (*14*). In the present study, the surface tensions and electrical conductivities of MSCN (M = Na, K, Rb, and Cs) melts were measured following the previous work, in which molten LiSCN was excepted because of its thermoliability.

Experimental Section

Materials. Chemicals used for the present studies were >99.9% pure (Rare Metal Co., Ltd.) and were dried at the temperatures 30 K below their melting points (*6*, *9*, *10*) under a reduced pressure of 0.13 Pa for 8 h.

Surface Tension. For the measurements of the surface tension the maximum bubble pressure method was applied because of its precision at high temperatures. Argon was used as a working gas, and it was purified by passing though chemical traps filled with molecular sieves (4A) and titanium sponges at 1173 K to remove possible H_2O, N_2, and O_2 contaminations. Pressure fluctuations of the gas were buffered by two 5-dm^3 buffer tanks. The gas flow was adjusted with a needle valve. A fused-silica tube was attached to a micrometer screw. A capillary tube of Pt–10% Rh alloy (2-mm outer diameter, 0.2 mm thick, 80 mm long) sharpened to a knife edge at the tip was attached to the lower end of the silica tube with a graphite joint. A manometer filled with *n*-butyl phthalate colored red by a dyestuff and kept at 303.5 ± 0.1 K by thermostated water was used to measure the pressure of the working gas bubble. The temperature of the furnace was maintained within ±1 K with a controlling device, and the temperature of the melt was measured with a C.A. thermocouple sheathed with a fused-silica tube. A fused-silica crucible containing the sample was set in the furnace, and then the atmosphere in the furnace was exchanged with the working gas. A detailed procedure of the measurement was described elsewhere (*15*).

The inner diameter of the capillary tip was determined by a measurement of the surface tension of distilled water at room temperature, and its diameter at the elevated temperature was corrected by use of the coefficient of thermal expansion for the alloy (*16*).

According to Nissen and Carlsten (*17*), the surface tension, γ, of the melt is calculated from

$$\gamma = rg(hd_1 - id_2)/2 - d_2r^2g/3 - d_2{}^2r^3[12hd_1 - id_2] \qquad (1)$$

where $2r$ is the inside diameter of the capillary, g the acceleration due to gravity, h the height of manometer, d_1 the density of *n*-butyl phthalate, which was measured pycnometrically, d_2 the density of the melt, and i the depth of immersion into the melt of the capillary.

Prior to the measurements of the melt samples, the surface tensions of molten $NaNO_3$ and KNO_3 were measured to obtain the precision of this apparatus, and comparisons were made among the recommended values (*18*, *19*) and observed ones. At 673 K, percent departures for $NaNO_3$ and KNO_3 were found to be 0.29% and 0.21%, respectively. Similar trends in the percent departure were observed over the measured temperature ranges. The surface tensions of molten KNO_3 were also remeasured periodically, and in each case the agreement was well within a reasonable experimental error ($\pm 0.30 \times 10^{-3}$ N m^{-1}, ca. ±0.3%). These mean that the apparatus is reliable enough to evaluate the surface tension of molten salts with low melting points.

Electrical Conductivity. A conventional ac bridge method was used to measure resistance of the melt in addition to that measured in previous investigation (*20*). A variable capacitance was also introduced in a Wheatstone bridge arrangement to correct the capacity of the electrical double layer near the electrode surface. A block diagram of the conductivity ac-

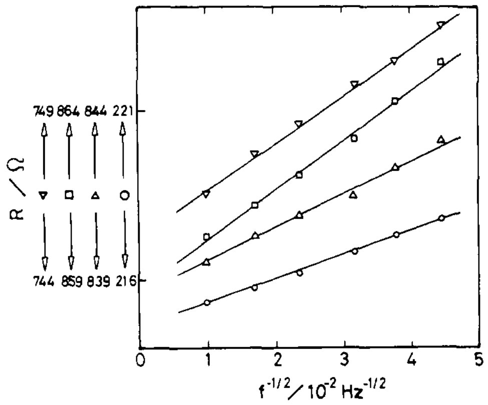

Figure 1. Resistance variation with frequency. ○, NaSCN at 604 K; △, KSCN at 474 K; □, RbSCN at 477 K; ▽, CsSCN at 521 K.

quisition system used is similar to that previously reported (*21*). The conductivity cell is of U-shaped type made of transparent fused silica, which has a capillary part of 3.5-mm inner diameter and 110-mm length. The disklike electrodes were made of platinum, with an area of about 1 cm^2. The so-called "gold furnace" was used to heat the samples, in which a Kanthal wire heater has been wound noninductively. This furnace has a uniform temperature distribution more than 100 mm in the center of furnace. Values of the resistance were corrected to take into account the resistance in the leads, which was measured in a separate experiment using a standard resistance. The cell constant was determined by using pure molten KNO_3, whose electrical conductivity was measured previously (*18*), before each experimental run. The value of 1.85×10^4 m^{-1} is satisfactorily large to obtain the electrical conductivity accurately, as pointed out by Janz et al. (*22*).

Tomkins et al. (*23*) have reported that the variation of resistance with frequency is expressed in the form

$$R_{\text{measd}} = R_{\text{inf}} + Cf^{-1/2} \qquad (2)$$

where R_{measd} and R_{inf} are the measured resistance at the frequency f and the polarization-free resistance at infinite frequency, respectively, and C is a constant characteristic of the melt studied. If the melt resistance and the faradaic impedance are assumed to be arranged in series for the equivalent circuit of the electrochemical process in the conductivity cell, the faradaic impedance consisting of a polarization resistance and an electrolytic capacitance is proportional to $f^{-1/2}$. For the melt samples, the relationship between the resistances and the applied frequencies from 0.5 to 10 kHz is indeed represented by a linear function of $f^{-1/2}$. Figure 1 shows that the relationship for each melt is obviously linear. Thus, the polarization-free resistance was obtained by extrapolating to infinity the frequency according to the above relationship.

The electrical conductivity of molten $NaNO_3$ was also measured to check the precision of the apparatus. The result showed the percent departures of −0.98% at 625 K and 0.28% at 673 K in comparison with the recommended values (*24*).

Results and Discussion

The surface tensions of MSCN melts are shown in Figure 2, and their numerical data are tabulated in Table I. The temperature ranges measured are limited near their melting points because of a thermodecomposition of the samples. In those ranges, the surface tensions decreased linearly with increasing temperature. Thus, the values were expressed as linear functions of temperature by least-squares fitting, with the results shown in Table II.

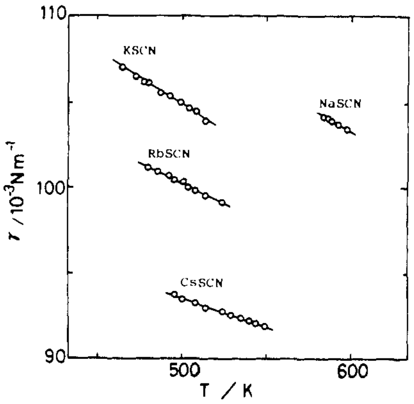

Figure 2. Surface tensions of molten thiocyanates.

Table I. Surface Tensions of Molten Thiocyanates

sample	T/K	$\gamma/10^{-3}$ N m^{-1}	sample	T/K	$\gamma/10^{-3}$ N m^{-1}
NaSCN	583	104.17		492	100.73
	586	104.10		495	100.41
	588	103.98		501	100.34
	592	103.78		504	99.94
	597	103.45		508	99.78
KSCN	464	107.00		514	99.55
	472	106.57		524	99.16
	477	106.22	CsSCN	496	93.66
	480	106.10		500	93.41
	487	105.60		508	93.21
	493	105.36		514	92.92
	499	105.05		524	92.68
	504	104.74		529	92.52
	508	104.51		535	92.36
	514	103.99		540	92.19
RbSCN	480	101.20		544	92.07
	485	100.96		549	91.87

Table II. Empirical Equations for Surface Tensions of Molten Thiocyanates[a]

$$\gamma = a - b \times 10^{-1}T$$

sample	a	b	SE[b]
NaSCN	134.92	0.5266	0.47×10^{-1}
KSCN	133.96	0.5807	0.65×10^{-1}
RbSCN	124.22	0.4796	0.93×10^{-1}
CsSCN	109.43	0.3196	0.47×10^{-1}

[a] $\gamma/10^{-3}$ N m^{-1}; T/K. [b] SE is the standard error of estimation.

As seen in Figure 2, the surface tensions of the MSCN evidently decreased with an increase of radii of the cations. This tendency is quite similar to those of molten halides and nitrates (*25*).

Surface energies, E^s/a, can be obtained from the surface tension by the equation

$$E^s/a = \gamma - T(\partial\gamma/\partial T) \qquad (3)$$

According to the equation, the surface energies become equal to the first term a in the surface tension equation since the surface tensions were represented by the linear function of temperature in K. These values are also close to those of nitrate melts with low melting points.

Frame et al. (*10*) have measured the surface tension of molten KSCN and reported that freshly prepared melt showed the temperature dependence of -1.36×10^{-3} N m^{-1} deg^{-1}, but after a certain time, the value changed to -0.14×10^{-3} N m^{-1} deg^{-1}. It has been described that a cause of such behavior would be attributed to bond rearrangements of SCN^- ions in the melt, i.e., formations of chainlike or ringlike polymerized ions. In this work, however, the behavior was not observed for the surface tension of all the melts measured. In addition, the reported values in both fresh and aged melts were found to be

Table III. Electrical and Equivalent Conductivities of Molten Thiocyanates

sample	T/K	$\kappa/10^2$ S m^{-1}	$\Lambda/10^{-4}$ S m^2 equiv^{-1}
NaSCN	597	0.6793	43.19
	601	0.6988	44.49
	604	0.7144	45.53
	609	0.7261	46.36
	614	0.7521	48.12
	617	0.7696	49.29
KSCN	474	0.1864	9.63
	483	0.2134	11.08
	492	0.2405	12.55
	502	0.2670	14.03
	508	0.2838	14.97
	413	0.2979	15.76
	519	0.3166	16.81
RbSCN	477	0.1746	12.56
	483	0.1794	12.93
	488	0.1965	14.19
	499	0.2194	15.91
	509	0.2403	17.47
	518	0.2610	19.04
CsSCN	501	0.2012	15.73
	506	0.2099	16.44
	512	0.2189	17.16
	516	0.2274	17.85
	522	0.2355	18.52
	527	0.2463	19.40

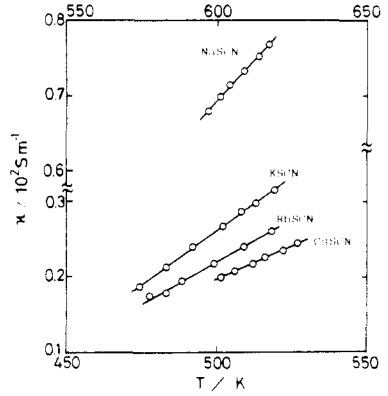

Figure 3. Electrical conductivities of molten thiocyanates.

Table IV. Electrical Conductivity Equations of Molten Thiocyanates[a]

$$\kappa = -a + b \times 10^{-3}T$$

sample	a	b	SE
NaSCN	1.8918	4.3084	0.40×10^{-2}
KSCN	1.1674	2.8581	0.11×10^{-2}
RbSCN	0.8646	2.1717	0.31×10^{-2}
CsSCN	0.6531	1.7049	0.10×10^{-2}

[a] $\kappa/10^2$ S m^{-1}; T/K.

Table V. Equivalent Conductivities of Molten Thiocyanates[a]

$$\Lambda = \Lambda_0 \exp(-E_a/RT)$$

sample	Λ_0	E_a
NaSCN	2141	19.36
KSCN	5515	24.96
RbSCN	2857	21.57
CsSCN	1032	17.42

[a] $\Lambda/10^{-4}$ S m^{-2}; E_a/kJ mol^{-1}.

lower by several 10^{-3} N m^{-1} than the observed ones of the KSCN in this study. If products based on the bond rearrangements are present in the melt, it is expected that they will be detected by spectroscopic studies such as Raman and IR spectra. However, observations of such products have not been reported (*1*, *2*, *26*).

Numerical data of the electrical conductivities for the MSCN are given in Table III, and their temperature dependences are shown in Figure 3. The electrical conductivities decreased in the sequence Na^+, K^+, Rb^+, Cs^+. In general, the electrical conductivity of molten salts is represented by a quadratic equation of the temperature. However, since in this work the measured temperature ranges are limited, a linear equation was applied. The results smoothed by the least-squares method are listed in Table IV.

The electrical conductivities of molten NaSCN and KSCN have been measured by Plester et al. (*9*) and Cingolani et al. (*12*). Both reported data were found to be larger by a few percent than our corresponding data.

The equivalent conductivities of the MSCN were computed from the numerical data in Table III and the molar volumes (*13*), V_m, by using the equation

$$\Lambda = \kappa V_m/n \tag{4}$$

where n is the valence of the component. The calculated values are listed in the third column of Table III. Since the ln Λ vs $1/T$ plots for the measured melts were straight lines, the equivalent conductivities were parameterized into the conventional Arrhenius-type equation

$$\Lambda = \Lambda_0 \exp(-E_a/RT) \tag{5}$$

where R is the gas constant in J K^{-1} mol^{-1} and Λ_0 and E_a are the frequency factor and the activation energy for conductivity, respectively. The calculations were carried out with the aid of least-squares fitting. The Λ_0 and E_a results are listed in Table V. The activation energies were similar to those of typical ionic melts.

It is well-known that the SCN^- ion easily forms complex compounds to metal atoms through S or N atoms (*2*). However, the results obtained from the present work indicate that if such tendencies are present in the molten state, the interactions must be very weak, so that the behavior of SCN^- ion in the melts is similar to that of the spherical anions of the alkali-metal halides in the molten state.

Acknowledgment

We express our sincere gratitude to H. Abe and Y. Ohya for assistance in measuring the electrical conductivities and the surface tensions.

Literature Cited

(1) Baddiel, C. B.; Janz, G. J. *Trans. Faraday Soc.* **1964**, *60*, 2009.
(2) Hester, R. E.; Krishnan, K. *J. Chem. Phys.* **1968**, *48*, 825.
(3) Ohno, H.; Igarashi, K.; Iwadate, Y.; Murofushi, M.; Mochinaga, M.; Furukawa, K. *Proceedings, Fifth International Symposium on Molten Salts*; Saboungi, M.-L., Johnson, K., Newman, D. S., Inman, D., Eds.; The Electrochemical Society: Pennington, NJ, 1986; p 296.
(4) Klug, H. P. *Z. Kristallogr., A* **1933**, *85*, 214.
(5) Akers, C.; Peterson, S. W.; Willett, R. D. *Acta Crystallogr.* **1968**, *B24*, 1125.
(6) Manolatos, S.; Tillinger, M.; Post, B. *J. Solid State Chem.* **1973**, *7*, 31.
(7) van Rooyen, P. H.; Boeyens, J. C. A. *Acta Crystallogr.* **1975**, *B31*, 2933.
(8) Irving, M. A.; Elcombe, M. M.; Smith, T. F. *Aust. J. Phys.* **1985**, *38*, 85.
(9) Plester, D. W.; Rogers, S. E.; Ubbelohde, A. R. *Proc. R. Soc. London* **1956**, *A235*, 469.
(10) Frame, J. P.; Rhodes, E.; Ubbelohde, A. R. *Trans. Faraday Soc.* **1959**, *55*, 2039.
(11) Jindal, H. R.; Harrington, G. W. *J. Phys. Chem.* **1967**, *71*, 1688.
(12) Cingolani, A.; Leones, D.; Lorenoti, A. *Ann. Chim.* **1977**, *67*, 97.
(13) Mochinaga, J.; Sasaki, Y.; Igarashi, K.; Suda, T. *Nippon Kagaku Kaishi* **1982**, 947.
(14) Iwadate, Y.; Kawamura, K.; Igarashi, K.; Mochinaga, J. *J. Phys. Chem.* **1982**, *86*, 5205.
(15) Igarashi, K.; Mochinaga, J. *Z. Naturforsch.* **1987**, *42a*, 690.
(16) Barter, B.; Darling, A. S. *Platinum Met. Rev.* **1960**, *4*, 138.
(17) Nissen, D. A.; Carlsten, R. W. *J. Electrochem. Soc.* **1974**, *121*, 500.
(18) Dahl, J. L.; Duke, F. R. *J. Phys. Chem.* **1958**, *62*, 1142.
(19) Janz, G. J. *J. Phys. Chem. Ref. Data* **1980**, *9*, 809.

(20) Iwadate, Y.; Igarashi, K.; Mochinaga, J.; Adachi, T. *J. Electrochem. Soc.* **1986**, *133*, 1162.

(21) Grjotheim, K.; Nikolic, R.; Øye, H. A. *Acta Chem. Scand.* **1970**, *24*, 489.

(22) Janz, G. J.; Krebs, U.; Siegenthaler, H. F.; Tomkins, R. P. T. *J. Phys. Chem. Ref. Data* **1972**, *1*, 584.

(23) Tomkins, R. P. T.; Janz, G. J.; Andalaft, E. *J. Electrochem. Soc.* **1970**, *117*, 906.

(24) King, L. A.; Duke, F. R. *J. Electrochem. Soc.* **1964**, *111*, 712.

(25) Janz, G. J.; Lakshminarayanan, G. R.; Tomkins, R. P. T.; Wong, J. Molten Salts Vol. 2. *Natl. Stand. Ref. Data Ser., Natl. Bur. Stand.* (*U.S.*) **1968**, *28*, 78–103.

(26) Ohno, K.; Igarashi, K.; Mochinaga, J.; Umesaki, N.; Iwamoto, N. *Proceeding of 19th Symposium on Molten Salts Chemistry*; Kozuka, Z., Ed.; The Molten Salt Committee of Electrochemical Society of Japan: Osaka, 1986; p 3.

Received for review August 11, 1988. Accepted March 28, 1989.

Solubility of Carbon Monoxide in Water–*n*-Butylamine, Ethanol–Cyclohexene, and Water–Dimethylformamide Mixtures

Mirza M. Taqui Khan,* Shivappa B. Halligudi, and Sumita Shukla

Homogeneous Catalysis Group, Coordination Chemistry Discipline, Central Salt & Marine Chemicals Research Institute, Bhavnagar 364 002, India

The solubility of carbon monoxide gas in water–*n*-butylamine, ethanol–cyclohexene, and water–dimethylformamide mixtures was experimentally determined by volumetric method using a 3×10^{-4} m^3 autoclave at three temperatures between 373 and 433 K. The solubility measurements have been made at two equilibrium pressures of CO for each set of mixtures at each temperature. The calculated Henry's constants have been correlated by use of the equation $\ln H = a + b/T$ for temperature dependence of CO solubility.

Introduction

Recent years have seen a marked trend in the application of many transition-metal complexes in catalyzed reactions of carbon monoxide to yield valuable chemicals (*1–3*). The predominant factors in these reactions are the feasibility and evaluation of optimum reaction conditions for the chosen catalyst systems to the desired products, and hence studies have been concentrated on these aspects. These reactions involve the interaction between gas and liquid and hence obviously are frequently limited by mass-transfer considerations. Studies on the kinetics of the high-pressure and high-temperature carbonylation reactions in the liquid phase catalyzed by soluble metal complexes necessarily involves knowledge of the solubility of CO in the liquid phase under experimental conditions. This would enable one to evaluate the kinetic rate constants and equilibrium constants involved in the mechanistic study of the reaction.

The CO solubility data that are needed for carbonylation reaction in the systems investigated by us are not known under the reaction conditions (*4*). To offset this, the present study was undertaken to provide data of CO solubility for water–*n*-butylamine, ethanol–cyclohexene, and water–dimethylformamide mixtures.

Experimental Section

The solubility apparatus and the method employed to determine CO solubilities are same as the one described by Chaudhary et al. (*5*). This volumetric method essentially involves the saturation of CO gas in a degassed solvent mixture at the desired partial pressure and temperature in an equilibrium cell (autoclave). A known volume of the saturated liquid is withdrawn after equilibration, and the amount of gas desorbed at room temperature and atmospheric pressure is measured by the volume of water displaced. Carbon monoxide gas of purity >99.96%, obtained from BOC, UK, was used. The solvents *n*-butylamine, ethanol, and dimethylformamide were of AR grade and distilled twice before use. Cyclohexene is prepared in our laboratory by the dehydration of cyclohexanol using concentrated sulfuric acid (*6*), and its purity checked by GLC was 99.8%. The autoclave of 3×10^{-4} m^3 volume used as equilibrium cell was procured from Parr Instrument Co., USA.

From a known amount of saturated liquid withdrawn after equilibration from the autoclave, the solubility of CO was calculated from the observed volume of the desorbed gas:

$$S = \frac{V - V_1}{V_1}\left[\frac{P - P_w - h/13.6}{101.3}\right]\frac{273}{T_w} + S_1 \qquad (1)$$

The solubility of CO is determined for the three systems studied at two different CO equilibrium pressures, and the average value after expressing in Henry's coefficient (*H*) was found to be reproducible within ±2–3% experimental error.

The vapor pressures of the mixtures required for CO partial pressure correction were determined in the same autoclave and used in the solubility calculations. This has the advantage that the value is known from practical measurements and no assumption using any equation need be made. This, we believe, will improve the accuracy of the results. The estimated errors in the present measurements of pressure, volume, and temperature were around ±3 kPa, $\pm 0.1 \times 10^{-6}$ m^3, and ±0.1 K, respectively.

Results and Discussion

The CO solubility data were obtained experimentally for CO–water–*n*-butylamine, CO–ethanol–cyclohexene, and CO–water–dimethylformamide systems in the temperature range 373–433 K at two equilibrium CO pressures (5×10^2–25×10^2 kPa). The solubilities (*S*) of CO estimated have been expressed in kmol/m^3. The effect of temperature and mole fraction change of one of the components of the mixtures on CO solubility was determined for the three systems, and these results

0021-9568/89/1734-0353$01.50/0